New Journal of Physics
The open access journal at the forefront of physics

Deutsche Physikalische Gesellschaft DPG IOP Institute of Physics

PAPER • OPEN ACCESS

Nonlinear quantum metrology with moving matter-wave solitons

To cite this article: D V Tsarev *et al* 2019 *New J. Phys.* **21** 083041

View the article online for updates and enhancements.

IOP ebooks™

Bringing you innovative digital publishing with leading voices to create your essential collection of books in STEM research.

Start exploring the collection - download the first chapter of every title for free.

This content was downloaded from IP address 95.55.137.51 on 24/08/2019 at 13:08

New Journal of Physics
The open access journal at the forefront of physics

Deutsche Physikalische Gesellschaft DPG
IOP Institute of Physics

Published in partnership with: Deutsche Physikalische Gesellschaft and the Institute of Physics

OPEN ACCESS

RECEIVED
21 May 2019

REVISED
29 July 2019

ACCEPTED FOR PUBLICATION
8 August 2019

PUBLISHED
22 August 2019

Original content from this work may be used under the terms of the Creative Commons Attribution 3.0 licence.

Any further distribution of this work must maintain attribution to the author(s) and the title of the work, journal citation and DOI.

PAPER

Nonlinear quantum metrology with moving matter-wave solitons

D V Tsarev[1], **T V Ngo**[1], **Ray-Kuang Lee**[2,3] **and A P Alodjants**[1]

[1] National Research University for Information Technology, Mechanics and Optics (ITMO), St. Petersburg 197101, Russia
[2] Physics Division, National Center for Theoretical Sciences, Hsinchu 30013, Taiwan
[3] Institute of Photonics Technologies, National Tsing Hua University, Hsinchu 30013, Taiwan

E-mail: alexander_ap@list.ru

Keywords: Bose–Einstein condensate, solitons, quantum metrology, *N*00*N*-state, Heisenberg limit, Fisher information

Abstract

The estimation of some parameters with super-Heisenberg (SH) sensitivity, i.e. beyond Heisenberg limit, is one of the principal problems for current quantum metrology. We propose to use Bose–Einstein condensate quantum bright solitons for this purpose. We have shown that solitons, as quantum nonlinear structured field objects, allow SH phase estimation even with coherent probes in the framework of a nonlinear metrology approach. To achieve ultimate scaling in nonlinear phase estimation, which is $1/N^3$, we examine soliton phase shift occurring due to interaction of weakly coupled 1D solitons. We have shown that steady states of coupled solitons can be used for the formation of maximally path-entangled *N*00*N*-state providing minimal propagation error of solitons' relative distance, momentum, and atom–atom scattering length parameter.

1. Introduction

Over the past decade, rapidly growing experimental facilities in quantum technologies have led to an increasing interest in quantum metrology and sensing [1, 2]. Many important applications, such as gravitational waves detection interferometers [3], frequency standards and atomic clocks [4, 5], magnetometers [6], quantum gyroscopes [7], thermometry of living cells [8], or high resolution imaging in biology [9] require to achieve ultimate sensitivity for some vital parameters, defined by quantum limitations of measurement accuracy. The measuring schemes, which should be highly phase-sensitive, propose an estimation of the phase shift containing all the information about the required parameter, see [10, 11].

In quantum optics, measurements for metrological purposes typically base on Mach–Zehnder interferometers operating with few photons (discrete variables) or with bright light beams containing a large average number of photons (so-called continuous variables [9]). In atomic optics domain, matter-wave interferometers commonly explore two internal state operations corresponding to a two-mode optical interferometer design [1].

Previously it was shown (see e.g. [12]) that two weakly coupled Bose–Einstein condensates (BEC) represent a versatile platform for metrological purposes in the framework of linear phase-sensitive measurements. In particular, Josephson and Fock regimes of interacting condensates allow to enhance accuracy of phase measurement beyond standard quantum limit (SQL), $1/\sqrt{N}$, where N is an average number of particles involved in a measurement scheme. Moreover, it was shown that so-called Heisenberg limit, N^{-1}, might be saturated with maximally entangled N-particle *N*00*N*-state in the framework of two-mode model approach [13, 14]. In this sense, *N*00*N*-state produced with a moderate number of particles represents a vital problem for current metrology and sensing. Some proposals are realized with a few number of particles [15–18]. The formation of robust *N*00*N*-states with atomic condensates is discussed in [19–21] where authors proposed to use two-site Bose–Hubbard model that is valid under some physical conditions for interacting condensates [22].

In [23] we examined weakly coupled one dimensional matter-wave bright solitons operating in a non-moving regime. We have shown that soliton superposition, *N*00*N*-state, is formed in the limit of Schrödinger-cat state only under certain requirements on parameters of the system. The sensitivity beyond Heisenberg limit was predicted.

© 2019 The Author(s). Published by IOP Publishing Ltd on behalf of the Institute of Physics and Deutsche Physikalische Gesellschaft

In this sense it is important to answer the question: can we obtain any benefits for metrological purposes with interacting condensates considered beyond two-mode approximation? In other words, what is the fundamental limit for the phase estimation and measurement if we use quantum field structures like solitons?

Before we answer these questions in the paper, some important features of solitons in quantum domain are worth mentioning. In particular, quantum field theory predicts that the average value of quantum soliton field amplitude represents superposition of classical solitons having different phase velocities [24]. Physically, it means that nonlinear phase contribution to quantum soliton behavior is non-trivial: the phase self-modulation compensates dispersion only on average, see [24]. The squeezing effect of quantum fluctuations and entanglement manifest this behavior, see [25, 26].

Strictly speaking, considering quantum solitons we deal with nonlinear quantum metrology approach based on many-body interactions [27, 28]. The nonlinear phase shift is the subject of measurement and estimation in this case [29, 30]. It is shown that super-Heisenberg (SH) scaling, which is beyond Heisenberg limit, might be attained even with coherent (semiclassical) probes [31].

The material of the paper is arranged as follows. In section 2 we consider ultimate scaling for nonlinear phase estimation accessible with quantum matter-wave soliton which we map onto single-mode (Goldstone) Hamiltonian. In section 3 we represent quantum field theory of moving solitons suitable for metrological purposes. We analyse various dynamical regimes for that. In section 4 the conditions and prerequisites of $N00N$-state formation with matter-wave solitons are established. Soliton coordinate and momentum represent new additional variables in this case which introduce some new important peculiarities in the measurement procedure of phase characteristics in the framework of quantum metrology. The sensitivity of coupled solitons' parameters estimation is discussed in section 5. In section 6 we summarize the results obtained.

2. Quantum solitons as a metrological tool

We start with the description of BEC given in Heisenberg representation. The dimensionless Hamiltonian describing dilute 1D atomic condensate looks like

$$\hat{H} = \int \mathrm{d}x \hat{\psi}^{\dagger}(x,\, t)\left(-\frac{1}{2}\frac{\partial^2}{\partial x^2} - \frac{u}{2}\hat{\psi}^{\dagger}(x,\, t)\hat{\psi}(x,\, t) + U_{\mathrm{tr}}(x)\right)\hat{\psi}(x,\, t), \tag{1}$$

where $\hat{\psi}(x,\, t)$ ($\hat{\psi}^{\dagger}(x,\, t)$) is a quantum field annihilation (creation) operator obeying bosonic commutation relations. We suppose that condensate is strongly trapped in the transverse yz plane that implies 2D harmonic potential, and $U_{\mathrm{tr}}(x)$ is a trapping potential in the third x dimension that is of our interest. In equation (1) $u = 2\pi|a_{\mathrm{sc}}|/a_0$ characterizes Kerr-like atomic nonlinearity, a_{sc} is an s-wave scattering length (in the paper we focus on attractive particles with negative scattering length which is already accounted in (1)), $a_0 = \sqrt{\hbar/m\omega_0}$ is a characteristic trap size and ω_0 is a harmonic trap frequency in a radial direction. All the variables in (1) are given in dimensionless units. In particular, all space variables are normalized on a_0: $x,\, y,\, z \rightarrow x/a_0,\, y/a_0,\, z/a_0$, and time is normalized on ω_0: $t \rightarrow \omega_0 t$.

For a moderate number of particles $\hat{\psi}(x,\, t)$ admits factorization [19]

$$\hat{\psi}(x,\, t) = \hat{a}(t)\Psi(x), \tag{2}$$

where $\hat{a}(t)$ is a time dependent operator characterizing quantum properties of a single condensate mode, $\Psi(x)$ is a C-number responsible for condensate spatial distribution, which is taken independent on N.

Notice that quantization of condensate field implies quantization of particle number operator defined as

$$\hat{N} = \hat{a}^{\dagger}\hat{a}. \tag{3}$$

Substituting (2) into (1) and using (3) for effective (single quantum mode) Hamiltonian one can obtain:

$$\hat{H}_{\mathrm{eff}} = \hbar\Omega_L\hat{N} - \hbar\Omega_2\hat{N}^2, \tag{4}$$

where we defined

$$\hbar\Omega_L = \int \mathrm{d}x\Psi^{*}(x)\left(-\frac{1}{2}\frac{\partial^2}{\partial x^2} + U_{\mathrm{tr}}(x)\right)\Psi(x), \tag{5}$$

$$\hbar\Omega_2 = \frac{u}{2}\int \mathrm{d}x|\Psi(x)|^4. \tag{6}$$

Equations (4)–(6) reflect a commonly used approach to condensate dynamical description if spatial degree of freedom is reduced [12, 19, 21, 22, 32]. The numerical values of condensate parameters in (5), (6) can be obtained via Gaussian variational anzatz for $\Psi(x)$ wave-function.

Let us now examine bright (non-moving) soliton solution case. At first, it is instructive to examine the problem in classical limit. Classical (C-number) description implies convenient Gross–Pitaevskii equation

$$\mathrm{i}\frac{\partial}{\partial t}\psi = -\frac{1}{2}\frac{\partial^2}{\partial x^2}\psi - u\,|\psi|^2\psi \tag{7}$$

obtained for condensate 'wave-function' $\hat{\psi}(x,\,t) \mapsto \psi(x,\,t)$ if condensate fluctuations are completely neglected [32]. The bright (non-moving) soliton solution of equation (7) is (see (2))

$$\psi(x,\,t) = \frac{N\sqrt{u}}{2}\,\mathrm{sech}\left[\frac{Nux}{2}\right]\mathrm{e}^{\mathrm{i}\frac{N^2u^2}{8}t}, \tag{8}$$

and obey normalization condition, $\int|\psi|^2\mathrm{d}x = N$, where $N = \langle\hat{N}\rangle$ is an average particle number. In the framework of field theory it is possible to consider classical Hamilton function corresponding to equation (7) with $U_{\mathrm{tr}} = 0$, which looks like (see [33])

$$H = \int \mathrm{d}x\psi^*(x,\,t)\left(-\frac{1}{2}\frac{\partial^2}{\partial x^2} - \frac{u}{2}|\psi(x,\,t)|^2\right)\psi(x,\,t). \tag{9}$$

Substituting equation (8) into (9) we immediately obtain

$$H = -\frac{N^4u^3}{32}\int \mathrm{d}x\left(\tanh^2\left[\frac{Nux}{2}\right]\mathrm{sech}^2\left[\frac{Nux}{2}\right]\right). \tag{10}$$

Performing integration in (10) we get $H = -\frac{N^3u^2}{24}$. Then taking into account quantization condition (3) one can represent corresponding Hamiltonian operator as

$$\hat{H}_{\mathrm{eff}} = -\hbar\Omega_3\hat{N}^3, \tag{11}$$

where

$$\hbar\Omega_3 = \frac{u^2}{24}. \tag{12}$$

Thus, equation (11) represents effective (single mode) Hamiltonian in quantum domain for bright soliton solution, see (4)–(6). One can see that the nonlinear structure of soliton field provides much higher power in respect to condensate quantum field (mode) operators $\hat{a}^\dagger$ and $\hat{a}$, see (4) and (11).

In the framework of quantum metrology we are interested in precise estimation of some parameter χ bounded by a quantum Cramer–Rao bound [34, 35]

$$\Delta\chi \geqslant \frac{1}{\sqrt{\nu}\sqrt{F_Q}}, \tag{13}$$

where ν is a number of experimental runs, F_Q is a quantum Fischer information. Without loss of generality, the unknown value $\chi \simeq \Omega_j$ might be inferred from the measurement procedure characterized by a unitary operator $\hat{U}_\chi = \exp[\mathrm{i}\chi\hat{G}]$, where $\hat{G}$ is a generator of state transformation. In the case of pure states, the Fisher information is characterized by dispersion of $\hat{G}$ [30]. As a result, one can show that for enough small $\chi \ll 1$ and $\hat{G} = \hat{N}^k$, the χ-parameter estimation scales as

$$\Delta\chi \propto \frac{1}{N^k}. \tag{14}$$

Thereafter we remove $\sqrt{\nu}$-factor for simplicity.

It follows from (14), that ultimate precision of measurement a condensate effective energy, $\chi = \Omega_0$, determined by (4) is

$$\Delta\chi = \frac{1}{N}, \tag{15}$$

which clearly corresponds to familiar Heisenberg limit [35].

An accurate measurement of $\chi = \Omega_2 \simeq u$—parameter according to its definition in (6) for nonlinear ('Kerr-like') phase shift implies maximal scaling

$$\Delta\chi = \frac{1}{N^2}. \tag{16}$$

It is important that one can surpass the Heisenberg limit (15) and obtain $\Delta\chi \propto 1/N^{3/2}$ measuring nonlinear phase shift with coherent probes, see (16) and [31].

The equation (14) demonstrates one important result of this paper for quantum solitons considering them in a single mode approximation: maximal scaling is

$$\Delta\chi = \frac{1}{N^3}, \tag{17}$$

which is obtained from (14) with $k = 3$, see (4).

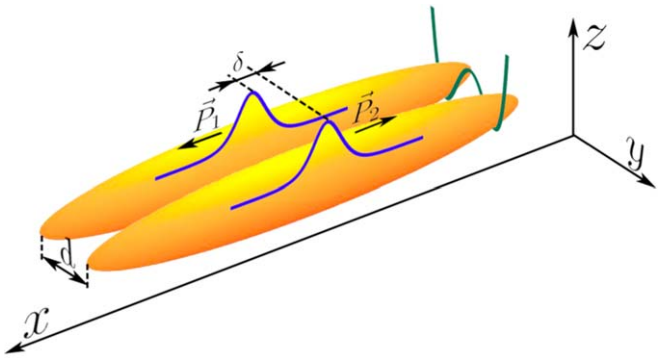

Figure 1. A sketch of counter-propagating matter-wave bright solitons with momenta $\overrightarrow{|P_1|} = \overrightarrow{|P_2|} = P/2$ and relative distance δ which are measured via solitons' nonlinear relative phase estimation. The platform is represented by two highly asymmetric (cigar-shape) condensates which are trapped in a double-well potential. d is the distance between trap centers, it can be explored by tailoring tunneling rate, κ.

3. Quantum model of coupled matter-wave solitons

3.1. Quantum field approach

From the practical point of view it is more convenient to consider an interferometer consisting of two-mode condensate trapped in a double-well potential [23]. The Hamiltonian of the system under consideration is

$$\hat{H} = \hat{H}_1 + \hat{H}_2 + \hat{H}_{\rm int}, \tag{18a}$$

where $\hat{H}_j\,(j = 1, 2)$ is the Hamiltonian for condensate particles in jth well, see (1); while $\hat{H}_{\rm int}$ accounts the inter-well coupling between two sites. In the second quantization form we explicitly have

$$\hat{H}_j = \int {\rm d}x \hat{\psi}_j^{\dagger}(x)\left(-\frac{1}{2}\frac{\partial^2}{\partial x^2} - \frac{u}{2}\hat{\psi}_j^{\dagger}(x)\hat{\psi}_j(x)\right)\hat{\psi}_j(x); \tag{18b}$$

$$\hat{H}_{\rm int} = \kappa \int {\rm d}x \hat{\psi}_2^{\dagger}(x)\hat{\psi}_1(x) + {\rm h.c.}, \tag{18c}$$

where κ denotes the inter-well tunneling rate and depends on the distance between the traps, see figure 1.

Schrödinger picture is more suitable for the analysis of the system described by (18). Further we restrict ourselves by the Hartree approach justified in a large particle number limit [23]. The N-particle ground state vector, $|\Psi\rangle_N$, can be written in this case as a product of N single-particle states

$$|\Psi\rangle_N = \frac{1}{\sqrt{N!}}\left[\int_{-\infty}^{\infty}(\Psi_1\hat{\psi}_1^{\dagger} + \Psi_2\hat{\psi}_2^{\dagger}){\rm d}x\right]^N|0\rangle, \tag{19}$$

where $|0\rangle \equiv |0\rangle_1|0\rangle_2$ is a two-mode vacuum state; Ψ_1 and Ψ_2 are unknown time-dependent soliton 'wave-functions' for which normalization condition

$${}_N\langle\Psi|\Psi\rangle_N = \int_{-\infty}^{\infty}(|\Psi_1|^2 + |\Psi_2|^2){\rm d}x = 1 \tag{20}$$

is satisfied. In this case, the bosonic field annihilation operators act on the state vector (19) as follows:

$$\hat{\psi}_j|\Psi\rangle_N = \Psi_j\sqrt{N}\,|\Psi\rangle_{N-1},\ j = 1,\ 2. \tag{21}$$

We can find the functions Ψ_j by variational approach, conventionally used in the field theory [19]. In particular, using (19) and (21) with (18) we obtain the Lagrangian density of coupled condensates in the form:

$$L = \sum_{j=1}^{2}\left(\frac{\rm i}{2}[\Psi_j^*\dot{\Psi}_j - \dot{\Psi}_j^*\Psi_j] - \frac{1}{2}\left|\frac{\partial\Psi_j}{\partial x}\right|^2 + \frac{u(N-1)}{2}|\Psi_j|^4\right)$$
$$- \kappa(\Psi_1^*\Psi_2 + \Psi_1\Psi_2^*). \tag{22}$$

Notice that in (22) we have omitted the common factor, N, describing the mean total number of particles. It is a constant so, as a common factor of Lagrangian terms, it makes no contribution to soliton dynamics.

Varying (22) for the independent field variables Ψ_1 and Ψ_2, we obtain coupled equations

$${\rm i}\frac{\partial}{\partial t}\Psi_{1,2} = -\frac{1}{2}\frac{\partial^2}{\partial x^2}\Psi_{1,2} - uN|\Psi_{1,2}|^2\Psi_{1,2} + \kappa\Psi_{2,1}. \tag{23}$$

Since $N \gg 1$ in equation (23) we suppose that $N - 1 \approx N$.

Equation (23) in the limit of $\kappa = 0$ admit exact moving soliton solution, see (8):

$$\Psi_j = \frac{N_j}{2}\sqrt{\frac{u}{N}}\,\mathrm{sech}\left[\frac{uN_j}{2}(x - x_{0j} - P_j t)\right]\exp\left[\mathrm{i}\frac{N_j^2 u^2}{8}t - \mathrm{i}\frac{P_j^2}{2}t + \mathrm{i}P_j(x - x_{0j})\right], \tag{24}$$

where x_{0j} and P_j play the roles of jth soliton initial average center position and momentum, respectively. In equation (24) we use normalization condition $\int|\Psi_j|^2\mathrm{d}x = N_j/N$ that leads to (20).

3.2. Basic equations

We suppose that weak coupling between solitons does not change the form of soliton envelope for which we consider wave-function ansatz, see (24), in the form:

$$\Psi_j = \frac{N_j}{2}\sqrt{\frac{u}{N}}\,\mathrm{sech}\left[\frac{uN_j}{2}(x - X_j)\right]\mathrm{e}^{\mathrm{i}\theta_j + \mathrm{i}P_j(x - X_j)}, \tag{25}$$

where $N_j(t)$, $\theta_j(t)$, $X_j(t)$ and $P_j(t)$ are jth soliton's particle number, phase, coordinate and momentum, respectively, which now are time-depended (variational) parameters. Thereafter, using Galilean invariance, we examine soliton properties in the reference frame supposing $P_1 = -P_2$ in (25).

By plugging (25) into (22) and averaging it, one can obtain an effective Lagrangian

$$Ł \equiv \int_{-\infty}^{\infty} L\mathrm{d}x = -\dot{\theta}z + \frac{\dot{\delta}P}{2} - \frac{P^2}{4} + \kappa(\Lambda + I)z^2 - I\kappa, \tag{26}$$

where dots denote derivatives with respect to time t; $\delta = X_2 - X_1, P = P_2 - P_1, z = \frac{N_2 - N_1}{N}$ and $\theta = \theta_2 - \theta_1$ are new variables minimally required for characterization of solitons' dynamics; $\Lambda = \frac{N^2u^2}{16\kappa}$ is a vital parameter of the system. In (26) we omit common factors and constant terms unimportant here. In (26) we also made a definition

$$I = \int_{-\infty}^{\infty}\frac{\cos[\theta + 2Px'/uN]\mathrm{d}x'}{\cosh[x' - zuN\delta/4] + \cosh[zx' - uN\delta/4]}. \tag{27}$$

With the Lagrangian (26), one can obtain the following variational equations for canonically conjugate soliton parameters:

$$\dot{\theta} = \Lambda z - \frac{1}{2}\frac{\partial}{\partial z}[(1 - z^2)I]; \tag{28a}$$

$$\dot{z} = \frac{1}{2}(1 - z^2)\frac{\partial I}{\partial\theta}; \tag{28b}$$

$$\dot{\delta} = \frac{P}{2\kappa} + (1 - z^2)\frac{\partial I}{\partial P}; \tag{28c}$$

$$\dot{P} = -(1 - z^2)\frac{\partial I}{\partial\delta}, \tag{28d}$$

where dimensionless time $\tau = 2\kappa t$ is used.

4. Soliton dynamics

4.1. Small-amplitude oscillations

The set of equations (28) characterizes a model of interacting solitons in the presence of their motion, see [23, 36]. This motion introduces some new important features which might be practically useful in the case of quantum measurement realization.

We start our analysis from small-amplitude inter-well oscillations occurring for the condensate population imbalance, z, see [37]. Fortunately, in this limit it is possible to approximate functional (27) as:

$$I \approx \frac{2\pi\sin\left[\frac{P\delta}{2}\right](1 - 0.21z^2)\cos[\theta]}{\sinh[uN\delta/4]\sinh[2\pi P/uN]} \equiv I_0(P, \delta)(1 - 0.21z^2)\cos[\theta]. \tag{29}$$

Direct numerical analysis of I revealed the fact that (29) is valid within the domain $|z| < 0.2$ and $|P|, |\delta| < 0.1$ with a relative error about 1.5%. In this limit (28a) and (28b) read

$$\dot{\theta} = z(\Lambda + 1.21I_0\cos[\theta]); \tag{30a}$$

$$\dot{z} = -\frac{1}{2}I_0\sin[\theta]. \tag{30b}$$

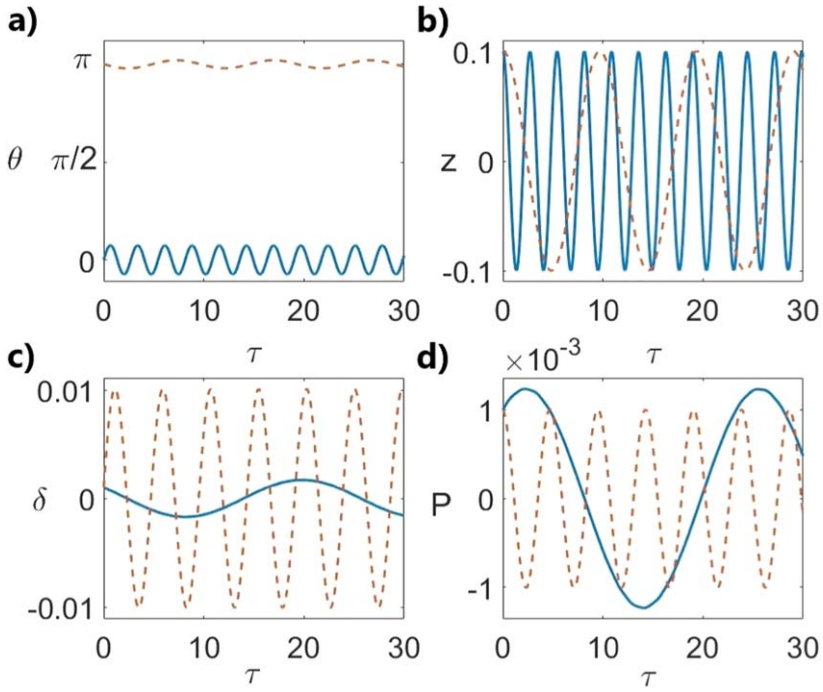

Figure 2. Phase difference (a), population imbalance (b), distance between solitons (c), and solitons' relative momentum (d) versus scaled dimensionless time τ for in-phase (blue solid curves) and out-of-phase (red dashed-and-dotted line) solitons' parameters with $\Lambda = 3$ and $\Lambda = 2$, respectively. The initial conditions are following: $z(0) = 0.1$, $\delta(0) = 10^{-3}$, $P(0) = 10^{-3}$, and $\kappa = 0.1$ in dimensionless units. The initial phase differences $\theta(0) = 0$ and $\theta(0) = \pi$ for the in-phase and out-of-phase solitons, respectively.

In (29) and (30) I_0 defines inter-well tunneling current amplitude, see [37]. If we additionally assume $P \ll 1$ and $\delta \ll 1$, then I_0 approaches

$$I_0 \approx 2\left(1 - \frac{u^2N^2\delta^2}{96} - \frac{2\pi^2P^2}{3u^2N^2}\right). \tag{31}$$

For numerical estimations we examine $^7_3$Li condensate containing $N \approx 10^3$ attractive particles. The scattering length, $a_{sc} = -1.45$ nm, is a tunable variable through Feshbach resonance [38, 39]. Trap characteristic length, $a_0 \approx 7$ μm, achieved with $\omega \approx 2\pi \times 29$ Hz. The condensate density in the trap center, $n = Na_0^{-3}$, in this case is about 3×10^{12} cm^{-3}. The particle interaction energy, $UN = \frac{2\pi\hbar^2 \mid a_{sc} \mid N}{ma_0^3 k_B}$, is 1.83 nK in temperature units and corresponds to $uN = UNk_B/\hbar\omega \approx 1.3$. The inter-well tunneling rate, $K = \hbar\omega\kappa/k_B = 0.14$ nK, implies $\kappa = 0.1$ and $\Lambda = 1$.

At first, we examine in-phase soliton dynamics with average (in time) phase behavior around $\theta \approx 0$, see the blue curves in figure 2. From (30) we obtain

$$\dot{\theta} = z(\Lambda + 2.42); \tag{32a}$$

$$\dot{z} = -\theta. \tag{32b}$$

Equations (32) describe small amplitude harmonic oscillations of the population imbalance, z, with a frequency $\omega_0 = \sqrt{(2.42 + \Lambda)}$, that is clearly seen in figure 2(b).

To examine temporal behavior of the distance between solitons, δ, and momentum, P, we combine (28c) and (28d) obtaining one second-order differential equation for δ:

$$\ddot{\delta} = \frac{1}{3}\delta\cos[\theta]\left(\Lambda - \frac{\pi^2}{3}\cos[\theta]\right) + z\frac{\pi^2}{6\kappa}P\sin[\theta]. \tag{33}$$

In (33) one can omit rapidly oscillating terms characterizing population imbalance, z, and phase difference, θ, see figures 2(a)–(d). As a result, we obtain

$$\ddot{\delta} = -\frac{1}{3}\left(\frac{\pi^2}{3} - \Lambda\right)\delta, \tag{34}$$

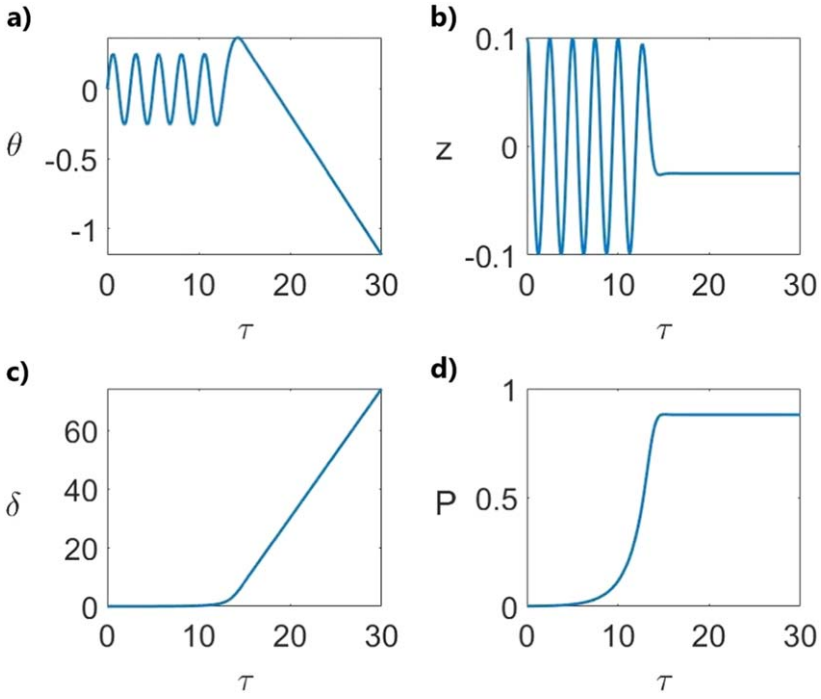

Figure 3. The same as in figure 2 but for the in-phase solitons with $\Lambda = 4$. Initial conditions are the same.

where $\Lambda_{cr} = \frac{\pi^2}{3} \approx 3.29$ is a critical value of parameter Λ relevant to soliton distance behavior. Particularly, in domain $\Lambda < \frac{\pi^2}{3}$, δ possesses small amplitude oscillations with frequency $\Omega_0 = \sqrt{\frac{1}{3}\left(\frac{\pi^2}{3} - \Lambda\right)}$ that is shown in figure 2(c) by the blue solid curve. Similar oscillatory behavior is inherent to P as it is seen from figure 2(d).

Otherwise, at $\Lambda > \frac{\pi^2}{3}$, solitons tend to separate, that is confirmed by numerical simulations of (28) and shown in figure 3. In particular, the distance between two solitons and their momentum difference exponentially grow and some certain population imbalance establishes as a result, see figures 3(b)–(d). Also notice that this dynamic regime is characterized by a running phase difference, θ.

Now let us switch our attention to the out-of-phase soliton interaction regime with average (in time) $\theta \approx \pi$. The red dashed lines in figure 2 demonstrate soliton parameter dynamics in this case. Small amplitude oscillations of z occur with frequency $\omega_\pi = \sqrt{(2.42 - \Lambda)}$, see figure 2(b). This solution is valid only for $\Lambda \leqslant 2.42$. Simultaneously, small-amplitude oscillations of δ and P happen with the frequency $\Omega_\pi = \sqrt{\frac{1}{3}\left(\frac{\pi^2}{3} + \Lambda\right)}$, see figures 2(c), (d).

Our estimations and figure 2 clearly demonstrate the important relations between characteristic frequencies which are $\omega_0/\omega_\pi > 1, \Omega_0/\Omega_\pi < 1$, see [37].

The analysis of (28) is quite complicated in a general case. Figure 4 reflects essentially nonlinear behavior of solitons' parameters. The dynamics starts from the running regime of the phase difference, figure 4(a). The parameters of the system correspond to self-trapping for population imbalance in this case. Then, the system enters to large amplitude (nonlinear) Rabi-oscillations shown in figure 4(b). The figure 4(a) shows that the phase, θ, admits oscillations in this case.

It is important to emphasize that these features of z and θ are inherent to moving solitons only and caused by the other soliton parameters influence, see [23, 36]. Actually, the parameters δ and P behave unstable and possess highly anharmonic but small amplitude persistent oscillations.

4.2. The steady-states

The set of equations (28) for static (non-moving) solitons admits steady-state solutions which are important for quantum measurement purposes [23]. Particularly, we are interested in an extreme case of the population imbalance, $z = \pm 1$. From (28) we have

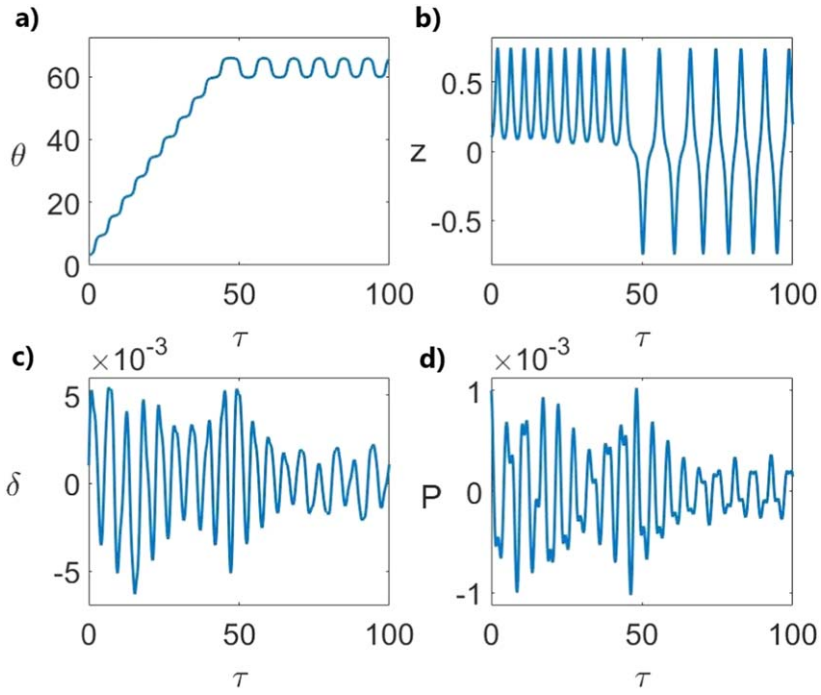

Figure 4. The same as in figure 2 but for the out-of-phase solitons with $\Lambda = 5$. Initial conditions are the same.

$$\dot{\theta} = (\Lambda + I)\,\mathrm{sign}(z); \tag{35a}$$

$$\dot{z} = 0; \tag{35b}$$

$$\dot{\delta} = \frac{1}{2\kappa}P; \tag{35c}$$

$$\dot{P} = 0. \tag{35d}$$

In this limit one can evaluate functional (27) analytically as

$$I = \frac{\pi}{2}\,\mathrm{sech}\left[\frac{\pi P}{uN}\right]\cos\left[\theta + \mathrm{sign}(z)\frac{P\delta}{2}\right] \approx A\cos[\theta] \tag{36}$$

with $A \equiv \frac{\pi}{2}\,\mathrm{sech}\left[\frac{\pi P}{uN}\right]\cos\left[\frac{P\delta_0}{2}\right]$. The last expression in (36) is valid for $\tau \ll \tau_{\mathrm{cr}} = 2\kappa\delta_0/P$. Thus, the measurement procedure should be performed within the time $t_{\mathrm{meas}} < \tau_{\mathrm{cr}}$. The numerical estimations performed for Lithium condensate solitons with $\delta_0 \simeq 0.1$ and $P \simeq 0.25$ lead to time $\tau_{\mathrm{cr}} \simeq 0.08$ which corresponds to experimentally accessible values of $\delta_0 \simeq 0.7\ \mu$m, $P \simeq 0.036\ \hbar\ \mu\mathrm{m}^{-1}$ and $t_{\mathrm{cr}} \simeq 2.16$ ms taken in physical units.

As a result, equation (36) can be taken as time-independent for small τ and steady-state solution of (35*a*) looks like

$$z_0^2 = 1; \tag{37a}$$

$$\theta_0 = \arccos[-\Lambda/A]. \tag{37b}$$

Notably, in the limit of non-moving solitons we put $P = 0$ in (37*b*) and the phase difference takes the form $\theta_0 = \arccos[-2\Lambda/\pi]$, see in [23].

5. Quantum measurements with traveling solitons

5.1. Projection measurement procedure

The results obtained in (37) with population imbalances, $z = \pm 1$, enable to consider a macroscopic quantum superposition $N00N$-state. Two 'halves' of the $N00N$-state can be obtained substituting $z = \pm 1$ into (25) and then into (19)

$$|\pm\rangle = \frac{1}{\sqrt{N!}}\left[\int_{-\infty}^{\infty}\Psi(x)\hat{\psi}_{2,1}^{\dagger}e^{\pm iPx/2}dx\right]^N|0\rangle, \tag{38}$$

where $\Psi(x) = \frac{\sqrt{Nu}}{2}\,\mathrm{sech}\left[\frac{Nu}{2}x\right]$. The $N00N$-state now represents a quantum superposition of (38):

$$|N00N\rangle = \frac{1}{\sqrt{2}}(|+\rangle + \mathrm{e}^{-\mathrm{i}N\theta_0}|-\rangle), \tag{39}$$

where we omitted the common phase factor $\mathrm{e}^{\mathrm{i}N\theta_2}$ and introduced the phase difference between two soliton states; θ_0 is the phase difference defined in (37*b*).

Note that equation (37*b*) is valid if inequality $\Lambda < |A|$ is fulfilled. Physically, this condition implies certain restrictions for Λ-parameter that determines $N00N$-state formation domain. In the limit of non-moving solitons, one gets $0 < \Lambda < \pi/2$. On the other hand, $N00N$-state formation becomes impossible since $A \to 0$ as far as $P \to \infty$.

Consider a projectile measurement procedure with state (39) introducing an operator (see [40]):

$$\hat{\Sigma} = |+\rangle\langle -| + |-\rangle\langle +|. \tag{40}$$

As a result, for the average value of Σ-operator (40), we obtain

$$\langle\hat{\Sigma}\rangle = \cos[N\theta_0] \tag{41}$$

with a dispersion

$$\langle(\Delta\hat{\Sigma})^2\rangle = \sin^2[N\theta_0]. \tag{42}$$

As seen from (41), the solitons' phase shift, θ_0, occurs in combination with a particle number, N, and as a result, is super-resolved. Actually, an arbitrary parameter, χ, relaying to θ_0 can now be estimated with sensitivity determined by the error propagation formula (see [41]):

$$\Delta\chi = \sqrt{\frac{\langle(\Delta\hat{\Sigma})^2\rangle}{\left|\frac{\partial\langle\hat{\Sigma}\rangle}{\partial\chi}\right|^2}} = \frac{1}{N}\left|\frac{\partial\theta_0}{\partial\chi}\right|^{-1}. \tag{43}$$

Factor N on the right-hand side in (43) indicates that the Heisenberg limit can be achieved if θ_0 depends on χ linearly. To overcome this limit, we use a nonlinear metrology approach, see [27, 28, 30].

5.2. Solitons' distance and momentum measurements

In general, the solitons' phase difference, θ_0, is a complicated quantity containing the information about atomic condensate material parameters, solitons' position, and momentum differences. Hence, these parameters might be subjects of estimation in a quantum domain. We start from accuracy of δ_0 or P-parameter measurements. Practically, such measurements seem to be actual in the framework of high resolution imaging and quantum lithography exploiting matter-wave peculiarities, see [13, 14]. The SQL of the measurements can be derived from the following simple arguments.

Suppose that the phase, θ, between two interfering counter-propagating atomic matter waves is $\theta = P\delta/\hbar$ (here we use actual physical units). The uncertainty in θ-measurement implies minimum detectable displacement $\Delta\delta = \hbar\Delta\theta/P$ at fixed P. the SQL of phase measurement is $\Delta\theta = 1/\sqrt{N}$, for displacement measurement we obtain

$$(\Delta\delta)_{\mathrm{SQL}} = \hbar/\sqrt{N}P. \tag{44}$$

Similar arguments bring us to the SQL formulation for momentum difference measurement

$$(\Delta P)_{\mathrm{SQL}} = \hbar/\sqrt{N}\delta. \tag{45}$$

It is important to stress that since the measurement time is small enough, we do not consider SQL occurring due to time dependent measurements for the soliton position and momentum, see [42].

Taking into account (37*b*) and definition (43), the solitons' position difference, $\chi \equiv \delta_0$, can be estimated with precision

$$\Delta\delta_0 = \frac{32\kappa}{N^3Pu^2}\left|\frac{\sqrt{A^2-\Lambda^2}}{\tan[P\delta_0/2]}\right|. \tag{46}$$

Figure 5 exhibits the dependence of $\sigma_\chi = \Delta\chi/\Delta\chi_{\mathrm{SQL}}$ on normalized particle number, $n = N/N_0$, where N_0 is a maximal average number of condensed atoms. It follows from figure 5 that SH sensitivity of δ_0 measurement occurs in the vicinity of points $n_{\min}$ and $n_{\max}$ when Λ approaches A (definition of n presumes $n_{\max} = 1$). The region between these points determines a domain of solution represented by equation (37*b*). This region decreases with increasing relative momentum, P. Particularly, if $P \to 0$, then $n_{\min} \to 0$; as a result we obtain $\Lambda_0 \to \pi/2$ that is a limit of non-moving solitons [23]. In the limit of $P \to \infty$, $n_{\min} \to 1$ and $\Lambda_0 \to 0$.

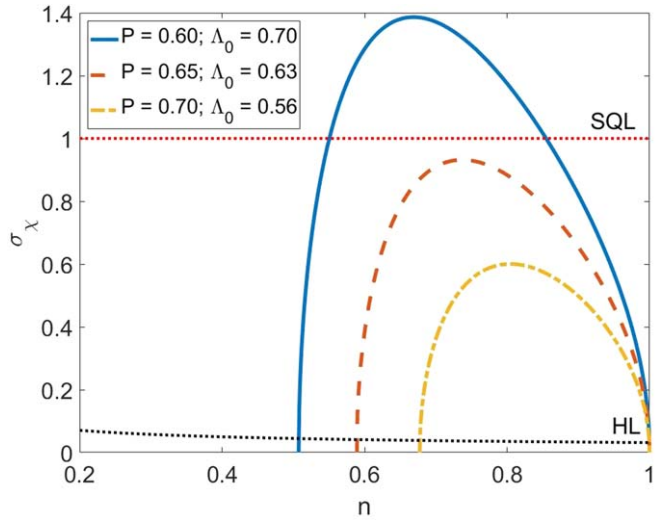

Figure 5. Error propagation for normalized relative coordinate measurement accuracy $\sigma_\chi = \Delta\chi/(\Delta\chi)_{\rm SQL}$ ($\chi \equiv \delta_0$) versus $n = N/N_0$. The parameters are following: $N_0 = 10^3$, $uN_0 = 1.3$ ($\Lambda_0 = A$), and $\delta_0 = 0.1$. Straight (red) line $\sigma_\chi = 1$ indicates measurement at SQL.

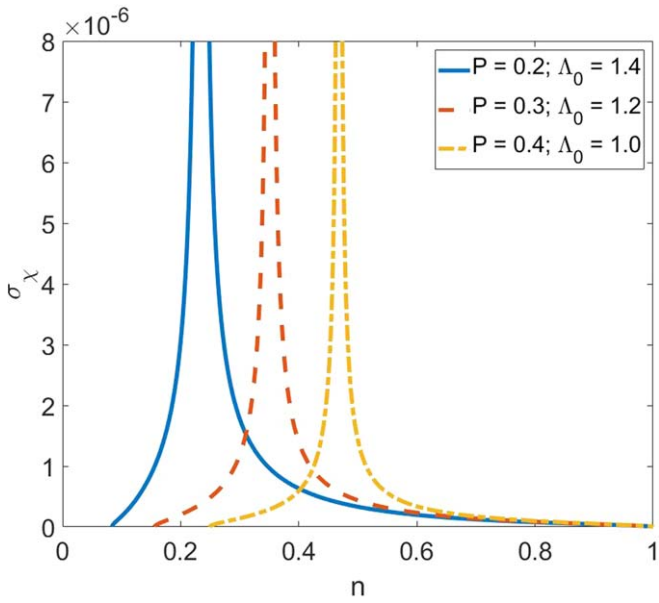

Figure 6. Error propagation for $\chi \equiv u^2$-parameter. The parameters are the same as in figure 5.

We can perform an estimation of soliton momentum difference in separate or subsequent measurements due to uncertainty relation that takes place for the quantum soliton coordinate and momentum [24]. The propagation error, ΔP, looks like

$$\Delta P = \frac{32\kappa}{N^3u^2}\left|\frac{\sqrt{A^2-\Lambda^2}}{\frac{2\pi}{uN}\tanh\left[\frac{\pi P}{uN}\right]+\delta_0\tan\left[P\delta_0/2\right]}\right|. \tag{47}$$

For $\delta_0 \ll \frac{2\pi}{uN} \approx 4.8$, equation (47) approaches

$$\Delta P = \frac{16\kappa}{\pi N^2u}\left|\frac{\sqrt{A^2-\Lambda^2}}{\tanh\left[\frac{\pi P}{uN}\right]}\right|. \tag{48}$$

Equation (48) is relevant to numerical estimations considered in the paper.

In the opposite limit, i.e. for $\delta_0 \gg \frac{2\pi}{uN}$, the equation (47) takes the form

$$\Delta P = \frac{32\kappa}{N^3 u^2 \delta_0} \left| \frac{\sqrt{A^2 - \Lambda^2}}{\tan\left[P\delta_0/2\right]} \right|. \tag{49}$$

Formally equation (49) predicts better scaling for momentum estimation than (48) if $P\delta_0/2$ is close to $\pi k/2$ ($k = 0, 1, 2, \ldots$). However in this case A-parameter tends to Λ and domain of accessible N collapses. In practice, equation (48) demonstrates better accuracy that obtained when $P\delta_0/2$ approaches πk.

5.3. Measurement of condensate material parameters

The soliton $N00N$-state (39) provides measurement of $\chi \equiv u^2$-parameter with error, see [23],

$$\Delta\chi = \frac{16\kappa}{N^3} \left| \frac{\sqrt{A^2 - \Lambda^2}}{1 - \frac{1}{2}\frac{\pi P}{Nu}\tanh\left[\frac{\pi P}{Nu}\right]} \right|. \tag{50}$$

The result obtained in (50) is in agreement with maximal scaling predicted in equation (17).

Figure 6 demonstrates SH sensitivity (50) of u^2 measurement performed with fixed (known) values of P, δ_0 and κ. It is important to stress that for experimentally accessible condensate parameters, all the curves are situated essentially below the Heisenberg limit. Equation (50) diverges when the denominator goes to zero. In this limit, we are not able to use equation (50) for our purposes. In this limit, we are not able to use equation (50) for our purposes, see figure 6.

6. Conclusion

In summary, we have theoretically studied the ultimate sensitivity of measurement of matter-wave quantum solitons' parameters using the nonlinear metrology approach. We have shown that nonlinear structured quantum fields, which are bright quantum solitons, provide a unique opportunity to achieve SH scaling ($\propto 1/N^{3/2}$) even with coherent probes. More accurate description of the problem being under discussion is based on the studies of two weakly-coupled elongated BECs trapped in a double-well potential in zy plane. Various dynamical regimes for solitons' parameters: population imbalance, relative phase, momentum, and coordinate, are examined in detail to elucidate experimentally accessible parameters for the estimation procedure. We have shown that steady-state solutions for population imbalance and phase difference exist within some parameters' window (at relatively short times) and provide maximally entangled $N00N$-state formation with moving quantum solitons. Then, we use soliton $N00N$-state to perform the estimation procedure of solitons' parameters by using the solitons' nonlinear relative phase. Particularly, the propagation measurement error of solitons' parameters, namely the relative coordinate and momentum, and u^2-parameter, proportional to atom–atom scattering length squared, scales as $1/N^3$. Applying these parameters' measurements for current quantum metrological purposes looks promising.

In the paper we have focused mostly on (projective) measurement procedure with soliton $N00N$-states to elucidate phase estimation beyond Heisenberg limit. Notably, the same SH limit might be attained with parity measurement scheme, see [23, 43]. Let us briefly discuss how to create $N00N$-states with solitons described above. We are confident that it is a non-trivial task and it opens new challenges both in theory and experiment. We find the protocol suggested in [20] the most suitable for these purposes. One can prepare $N00N$-state dynamically starting from the state $|\Psi(\theta(0))\rangle = \sum_{n=0}^{N} C_n e^{-in\theta(0)} |N - n, n\rangle$, where $|N - n, n\rangle$ is a two-mode Fock state, C_n characterizes initial (binomial) distribution, and $\theta(0)$ is an initial phase difference. Next, it is necessary to construct appropriate two-soliton Hamiltonian which is relevant to a two-mode approach in the framework of procedure described in equations (7)–(12) Then, applying an evolution operator with this Hamiltonian after some time interval (defined by characteristic parameters of solitons) one can obtain superposition (Schrödinger-cat or $N00N$) states like in equations (38), (39) Notably, as it was shown in [20], two halves of $N00N$-state are shifted by π in θ-phase domain which is in agreement with results that we exploit in equations (38), (39). Actually, the phase difference $\theta_0 = \theta_0(0)$ in (37b) represents a steady-state solution and goes to π in the non-moving solitons limit for critical value $\Lambda = 1.58$, see [23].

Obviously, decoherence and losses represent very important problem at the stage of $N00N$-state formation [20]. We discussed various aspects of this problem for non-moving quantum bright solitons in [23]. Many-body effects including single and two-body losses should be considered [44]. In forthcoming publications, we plan to examine the influence of these effects on our model in details.

Acknowledgments

This work was supported by Grants No 19-52-52012 and No 08-08 of RFBR and Government of Russian Federation, respectively. RKL was supported by the Ministry of Science and Technology of Taiwan (No 105-2628-M-007-003-MY4, No 107-2627-E-008-001, and No 108-2923-M-007-001-MY3).

ORCID iDs

D V Tsarev https://orcid.org/0000-0002-9041-2708

References

[1] Pezzè L, Smerzi A, Oberthaler M K, Schmied R and Treutlein P 2018 *Rev. Mod. Phys.* **90** 035005
[2] Degen C L, Reinhard F and Cappellaro P 2017 *Rev. Mod. Phys.* **89** 035002
[3] Schnabel R 2017 *Phys. Rep.* **684** 1–51
[4] Huelga S F, Macchiavello C, Pellizzari T, Ekert A K, Plenio M B and Cirac J I 1997 *Phys. Rev. Lett.* **79** 3865
[5] Ludlow A D, Boyd M M, Ye J, Peik E and Schmidt P O 2015 *Rev. Mod. Phys.* **87** 637–701
[6] Kitching J, Knappe S and Donley E A 2011 *IEEE Sens. J.* **11** 1749–58
[7] Berg P, Abend S, Tackmann G, Schubert C, Giese E, Schleich W P, Narducci F A, Ertmer W and Rasel E M 2015 *Phys. Rev. Lett.* **114** 063002
[8] Kucsko G, Maurer P C, Yao N Y, Kubo M, Noh H J, Lo P K, Park H and Lukin M D 2013 *Nature* **500** 54–8
[9] Taylor M A and Bowen W P 2016 *Phys. Rep.* **615** 1059
[10] Hentschel A and Sanders B S 2010 *Phys. Rev. Lett.* **104** 063603
[11] Kolodynski J and Demkowicz-Dobrzanski R 2013 *New J. Phys.* **15** 073043
[12] Pezzè L, Collins L A, Smerzi A, Berman G P and Bishop A R 2005 *Phys. Rev.* A **72** 043612
[13] Boto A N, Kok P, Abrams D S, Braunstein S L, Williams C P and Dowling J P 2000 *Phys. Rev. Lett.* **85** 2733
[14] Dowling J P 2008 *Contemp. Phys.* **49** 125–43
[15] Afek I, Ambar O and Silberberg Y 2010 *Science* **328** 879–81
[16] Rozema L A, Bateman J D, Mahler D H, Okamoto R, Feizpour A, Hayat A and Steinberg A M 2014 *Phys. Rev. Lett.* **112** 223602
[17] Merkel S T and Wilhelm F K 2010 *New J. Phys.* **12** 093036
[18] Chen Y A, Bao X H, Yuan Z S, Chen S, Zhao B and Pan J W 2010 *Phys. Rev. Lett.* **104** 043601
[19] Cirac J I, Lewenstein M, Mølmer K and Zoller P 1998 *Phys. Rev.* A **57** 1208
[20] Piazza F, Pezzè L and Smerzi A 2008 *Phys. Rev.* A **78** 051601(R)
[21] Mazzarella G, Salasnich L, Parola A and Toigo F 2011 *Phys. Rev.* A **83** 053607
[22] Anglin J R and Vardi A 2001 *Phys. Rev.* A **64** 013605
[23] Tsarev D V, Arakelyan S M, Chuang Y, Lee R K and Alodjants A P 2018 *Opt. Express* **26** 19583–95
[24] Lai Y and Haus H A 1989 *Phys. Rev.* A **40** 844–53
[25] Drummond P D, Shelby R M, Friberg S R and Yamamoto Y 1993 *Nature* **365** 307–13
[26] Lai Y and Lee R K 2009 *Phys. Rev. Lett.* **103** 013902
[27] Beau M and del Campo A 2017 *Phys. Rev. Lett.* **119** 010403
[28] Napolitano M and Mitchell M W 2010 *New J. Phys.* **12** 09301
[29] Cheng J 2014 *Phys. Rev.* A **90** 063838
[30] Maldonado-Mundo D and Luis A 2009 *Phys. Rev.* A **80** 063811
[31] Luis A 2007 *Phys. Rev.* A **76** 035801
[32] Parkins A S and Walls D F 1998 *Phys. Rep.* **303** 1–80
[33] Ablowitz M J and Segur H 1981 *Solitons and the Inverse Scattering Transform* (Philadelphia, PA: SIAM)
[34] Tóth G and Apellaniz I 2014 *J. Phys. A: Math. Theor.* **47** 424006
[35] Demkowicz-Dobrzański R, Jarzyna M and Kołodyński J 2015 *Prog. Opt.* **60** 345–435
[36] Raghavan S and Agrawal G P 2000 *J. Mod. Opt.* **47** 1155–69
[37] Smerzi A, Fantoni S, Giovanazzi S and Shenoy S R 1997 *Phys. Rev. Lett.* **79** 4950
[38] Bradley C C, Sackett C A and Hulet R G 1997 *Phys. Rev. Lett.* **78** 985
[39] Abraham E R I, McAlexander W I, Sackett C A and Hulet R G 1995 *Phys. Rev. Lett.* **74** 1315
[40] Kok P, Braunstein S L and Dowling J P 2004 *J. Opt.* B **6** S811
[41] Helstrom C W 1976 *Quantum Detection and Estimation Theory* (New York: Academic)
[42] Braginsky V B and Khalili F Y 1992 *Quantum Measurement* (Cambridge: Cambridge University Press)
[43] Gerry C C, Benmoussa A and Campos R A 2017 *J. Mod. Opt.* **54** 2177
[44] Czajkowski J, Pawlowski K and Demkowicz-Dobrzański R 2019 *New J. Phys.* **21** 053031